Food Chemistry: X 14 (2022) 100273

Contents lists available at ScienceDirect

Food Chemistry: X

journal homepage: www.sciencedirect.com/journal/food-chemistry-x

Treponema primitia α1–2-fucosyltransferase-catalyzed one-pot multienzyme synthesis of fucosylated oligosaccharide lacto-*N*-fucopentaose I with antiviral activity against enterovirus 71

Yuanyuan Liu [a,1], Aijun Tong [a,1], Xiaoxiang Gao [a], Sinan Yuan [a], Ruting Zhong [d], Chao Zhao [a,b,c,*]

[a] College of Food Science, Fujian Agriculture and Forestry University, Fuzhou 350002, China
[b] Engineering Research Centre of Fujian-Taiwan Special Marine Food Processing and Nutrition, Ministry of Education, Fuzhou 350002, China
[c] Key Laboratory of Marine Biotechnology of Fujian Province, Institute of Oceanology, Fujian Agriculture and Forestry University, Fuzhou 350002, China
[d] Institute of Chinese Medical Sciences, University of Macau, Taipa, Macau, China

ARTICLE INFO

Keywords:
Treponema primitia α 1–2-fucosyltransferase
One-pot multienzyme synthesis
Lacto-*N*-fucopentaose I
Anti-enterovirus 71

ABSTRACT

Fucosylated oligosaccharides have important biological functions as well as an excellent antiviral activity. A novel α 1–2-fucosyltransferase (α 2FT) from *Treponema primitia* (Tp2FT) was cloned and expressed in *Escherichia coli* BL21(DE3) and purified as an N-His_6-tagged fusion protein (His_6-Tp2FT). Mass spectrometry was carried out to identify the products of enzymatic reaction. The Tp2FT exhibited strict acceptor substrate specificity for type 1 structure (Galβ1-3GlcNAc)-containing glycans. It might be a promising emzyme for the chemo-enzymatic synthesis of lacto-*N*-fucopentaose I (LNFP I), which is one of the important fucosylated oligosaccharides. In this study, different *in vitro* experiments were used to study the biological activities of LNFP I. It could reduce the concentrations of inflammatory cytokines and effectively inhibit the synthesis of enterovirus 71 proliferation. LNFP I was an inhibitor of enterovirus 71 in the early stages of infection, it can used in infant nutrition and might provide a new drug for hand foot mouth disease.

1. Introduction

Fucosylated glycans have potential pharmaceutical applications, especially fucosylated human milk oligosaccharides. Lacto-*N*-fucopentaose I (LNFP I) is an important nutrient in breast milk, which has good functions of anti-norovirus, promoting the growth of intestinal probiotics, and preventing breast cancer metastasis (Derya et al., 2020). However, the chemical synthesis of LNFP I has not met an increase in its demand due to its low efficiency and yield. Due to the high specificity and efficiency of their enzymatic reactions, the enzymatic synthesis of LNFP I has become an effective alternative to chemical synthesis (Sprenger, Baumgärtner, & Albermann, 2017). Zhao et al. (2016) suggested the one-pot multienzyme (OPME) synthesis of fucosylated oligosaccharides with novel high-reactivity and low-substrate hydrolytic α 1–2-fucosyltransferase (α 2FT), which were obtained from *Thermosynechococcus elongatus*. The fucosyltransferase is one of the most important glycosyltransferases, which catalyzes the transfer of L-fucose from guanosine-5′-diphospho-β-fucose (GDP-fucose) to galactose (Gal) to form α 1–2-linkage, or to *N*-acetylglucosamine (GlcNAc) to form α 1–3-, α 1–4-, and α 1–6-linkages (Gnoth et al., 2000; Ruiz-Palacios et al., 2003; Wilson et al., 2017). The α 2FT-catalyzed synthesis does not need the chemical protection or de-protection of substrates because of its high substrate specificity and stereo-selectivity, providing a huge advantage for the synthesis of fucose-containing human milk oligosaccharides (Castanys-Muñoz, Martin, & Prieto, 2013; Lee et al., 2012). Therefore, the exploration of more special bacterial glycosyltransferases has very good prospects (Meints et al., 2017). The α 2FTs from humans, other mammals, viruses, plants, and bacteria belong to glycosyltransferase family 11 (GT11). Several of the genes responsible for the bacterial α 2FT have been cloned and identified, such as WbiQ, WbsJ, WbnK, Wbwk, WbgL, Hp2FT, Te2FT, and Ts2FT sequences from *Escherichia coli* O127:K63(B8), *E. coli* O128, *E. coli* O86:K62:H2, *E. coli* O86:B7, *E. coli* O126, *Helicobacter pyolori* FutC, *Thermosynechococcus elongates* BP-1, and *Thermosynechococcus* sp. NK55a, respectively (Baumgärtner, Seitz, Sprenger, & Albermann, 2013; Engels & Elling, 2014; Li, Liu et al., 2008, Li, Shen et al., 2008b; Pettit et al., 2010; Zhao et al., 2016; Zhong et al.,

* Corresponding author at: No. 15 Shangxiadian Rd., Fuzhou 350002, China.
E-mail address: zhchao@live.cn (C. Zhao).
[1] Yuanyuan Liu and Aijun Tong contributed equally to this study.

https://doi.org/10.1016/j.fochx.2022.100273
Received 1 November 2021; Received in revised form 20 February 2022; Accepted 24 February 2022
Available online 26 February 2022

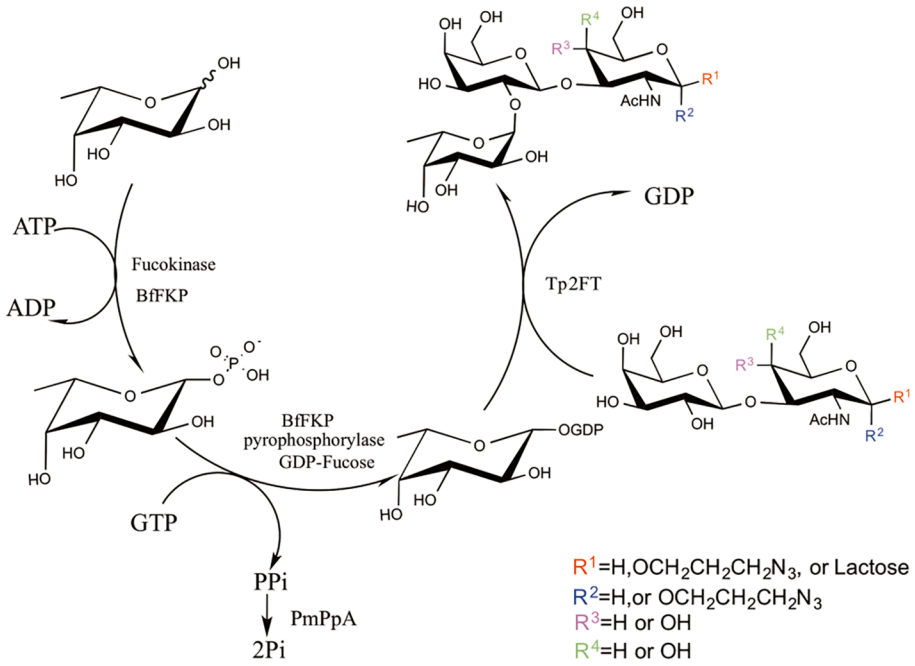

Fig. 1. Synthesis of α 1–2-fucosides with one-pot three-enzyme. BfFKP, *Bacteroides fragilis* strain NCTC9343 bifunctional L-fucokinase/GDP-fucose pyrophosphorylase; PmPpA, *Pasteurella multocida* inorganic pyrophosphorylase; and Tp2FT, *Treponema primitia* α 1–2-fucosyltransferase.

2022), and with low expression levels and different substrate specificity for each enzyme (Seydametova et al., 2019; Stein, Lin, & Lin, 2008; Wang et al., 1999; Zhao et al., 2017). Besides, *Helicobacter mustelae α* 1–2-fucosyltransferase (Hm2FT) has been cloned and used for enzymatic and chemoenzymatic synthesis (Xiao et al., 2016; Ye et al., 2019), but its biochemical characterization has not been reported.

Enterovirus 71 (EV71) is a member of the family Picornaviridae, and a major pathogen of hand-foot-mouth diseases (HFMD) (Lyu et al., 2015). It is highly contagious in the central nervous system and prone to a variety of neuro-related diseases, including aseptic meningitis, poliomyelitis-like paralysis, and brainstem encephalitis (McMinn, 2012). The EV71 has a single-plus-stranded RNA genome, which is composed of about 7408 nucleotides. The virus shell is composed of four shell proteins (VP1, VP2, VP3, and VP4), among which the VP1 is the most important for its determination as antigen (Gao et al., 2020). It can combine with appropriate compounds to stabilize the viral capsid and prevent the un-coating of virus and release of RNA (Smyth & Martin, 2002). The immune status of the body is regulated by the interactions between neuroendocrine and immune cells or their coordination with drugs. The immune response is maintained at the most appropriate level in the most appropriate form and maintains the steady-state of immune function. The mononuclear macrophages are present in all tissues and can protect against potential pathogens (Liu et al., 2017). They play a key role in non-specific immunity, and can also induce other immune cells, such as lymphocytes, to further initiate the specified defense mechanisms (Zhang & Wang, 2014). In this study, a novel *α* 2FT from *Treponema primitia* (Tp2FT) was discovered and its ability to synthesize the LNFP I were evaluated (Fig. 1). Moreover, the antiviral activity against EV71 and the anti-inflammatory activities in lipopolysaccharide (LPS)-induced mouse mononuclear macrophages (RAW264.7) of LNFP I were also investigated.

2. Materials and methods

2.1. Cloning and construction of His_6-Tp2FT recombinant vector

The primers used to clone Tp2FT included the following: 5′- CATATGATATTATTTTGGTC-3′ and 5′-GGATCCTTATTT ATCAATAACGAAG G-3′. A 50 μL PCR reaction included the following: 10 × Taq polymerase Buffer (5 μL), template DNA (1 μL), forward and reverse primers (1 μL each), dNTPs (1 μL), ddH_2O (40.5 μL), Taq polymerase (0.5 μL). The PCR conditions were as following: initial denaturation for 5 min at 94℃, followed by 30 cycles of denaturation for 1 min at 94℃, annealing for 40 s at 52℃, and extension for 2 min and 30 *sec* at 72℃, and final extension at 72℃ for 5 min. The PCR product and the vector plasmid pET15b were digested with *Nde*I and *BamH*I restriction enzymes and purified using the DNA Purification Kit (Beyotime, Shanghai, China). The recombinant expression vector was obtained by the ligation of the target gene with vector in the presence of DNA ligase. The recombinant plasmid was identified using DNA sequencing and a macro-restriction map. The screened positive plasmids were transformed into *E. coli* BL21 (DE3) chemically competent cells. After obtaining the recombinant expression vector, it was transferred into *E. coli*, which was grown on ampicillin medium.

2.2. Overexpression and purification His_6-Tp2FT

After the activation of *E. coli* BL21 strain containing the target gene, a colony was picked and cultured in Luria-Bertani (LB)-agar plate (100 μg/mL ampicillin, 10 g/L NaCl, 10 g/L tryptone, and 5 g/L yeast extract) at 37℃ for 14–16 h. The culture was inoculated in 500 mL fresh liquid medium using 1% inoculation amount. The culture was allowed to grow at 37℃ until the optical density (OD) at 600 nm reached 0.6. Then, 500 μL of isopropyl-1-thio-β-D-galactopyranoside (IPTG) (100 mM) was added to the medium and incubated at 16℃ for 20 h. The cells were then collected by centrifuging at 10,621 × *g* and 4℃ for 10 min. The cell pellet was re-suspended in lysis buffer (pH 8.0, 100 mM Tris-HCl, containing 0.1% Triton X-100) (30 mL/L cell culture) and the cells were lysed using sonication on ice (work 2 s, stop 3 s, last for 5 min). The cell lysate was then centrifuged at 17,949×*g* and 4℃ for 20 min, and then the supernatant was purified using a Ni-NTA column pre-equilibrated with 8 column volumes of binding buffer (5 mM imidazole, 0.5 M NaCl, 50 mM Tris-HCl, pH 7.5). The proteins were washed with 10 column volumes of washing buffer (50 mM imidazole, 0.5 M NaCl, 50 mM Tris-HCl, pH 7.5), and then eluted with elution buffer (200 mM imidazole, 0.5 M NaCl, 50 mM Tris-HCl, pH 7.5). The expression and

Table 1
Acceptor substrate specificity of His_6-Tp2FT. ND, no activity detected.

Acceptors	Products	Convert ratio %
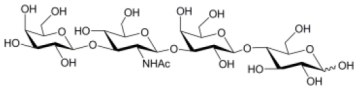 Galβ1–3GlcNAcβ1–3Galβ1–4Glc (***1***)	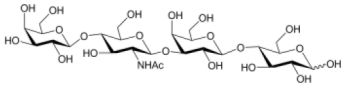 Fuc α 1–2-Galβ1–3GlcNAcβ1–3Galβ1–4Glc (***11***)	34.9
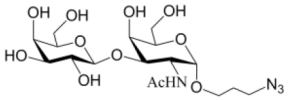 Galβ1–3GlcNAcβ1–3Galβ1–4Glc (***2***)	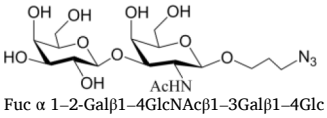 Fuc α 1–2-Galβ1–4GlcNAcβ1–3Galβ1–4Glc (***12***)	7.4
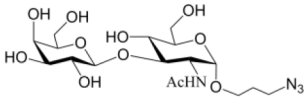 Galβ1–3GalNAc α $ProN_3$ (***3***)	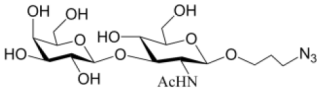 Fuc α 1–2-Galβ1–3GalNAc α $ProN_3$ (***13***)	20
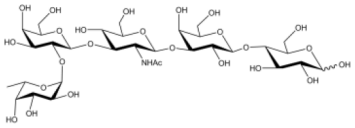 Galβ1–3GalNAcβ$ProN_3$ (***4***)	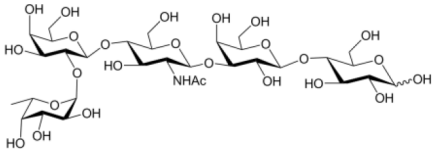 Fuc α 1–2-Galβ1–3GalNAcβ$ProN_3$ (***14***)	10.7
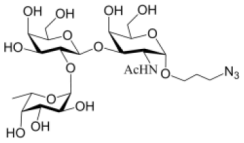 Galβ1–3GlcNAc α $ProN_3$ (***5***)	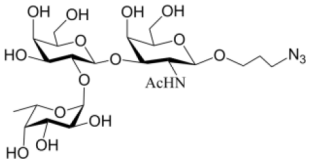 Fuc α 1–2-Galβ1–3GlcNAc α $ProN_3$ (***15***)	28.2
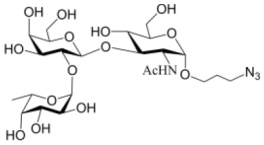 Galβ1–3GlcNAcβ$ProN_3$ (***6***)	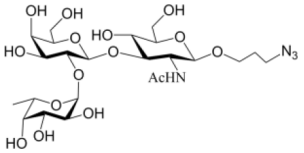 Fuc α 1–2-Galβ1–3GlcNAcβ$ProN_3$ (***16***)	94.1
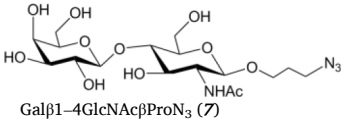 Galβ1–4GlcNAcβ$ProN_3$ (***7***)	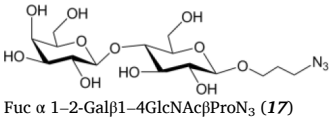 Fuc α 1–2-Galβ1–4GlcNAcβ$ProN_3$ (***17***)	ND
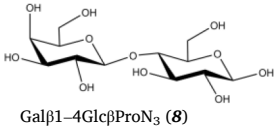 Galβ1–4GlcβProN_3 (***8***)	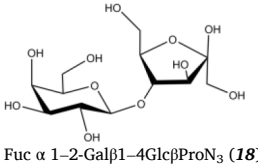 Fuc α 1–2-Galβ1–4GlcβProN_3 (***18***)	ND
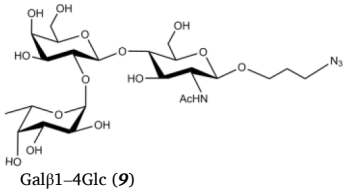 Galβ1–4Glc (***9***)	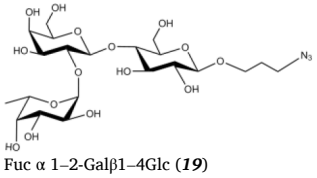 Fuc α 1–2-Galβ1–4Glc (***19***)	ND
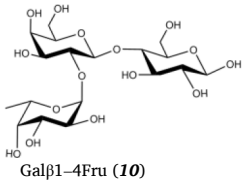 Galβ1–4Fru (***10***)	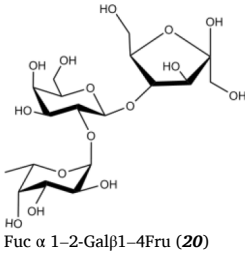 Fuc α 1–2-Galβ1–4Fru (***20***)	ND

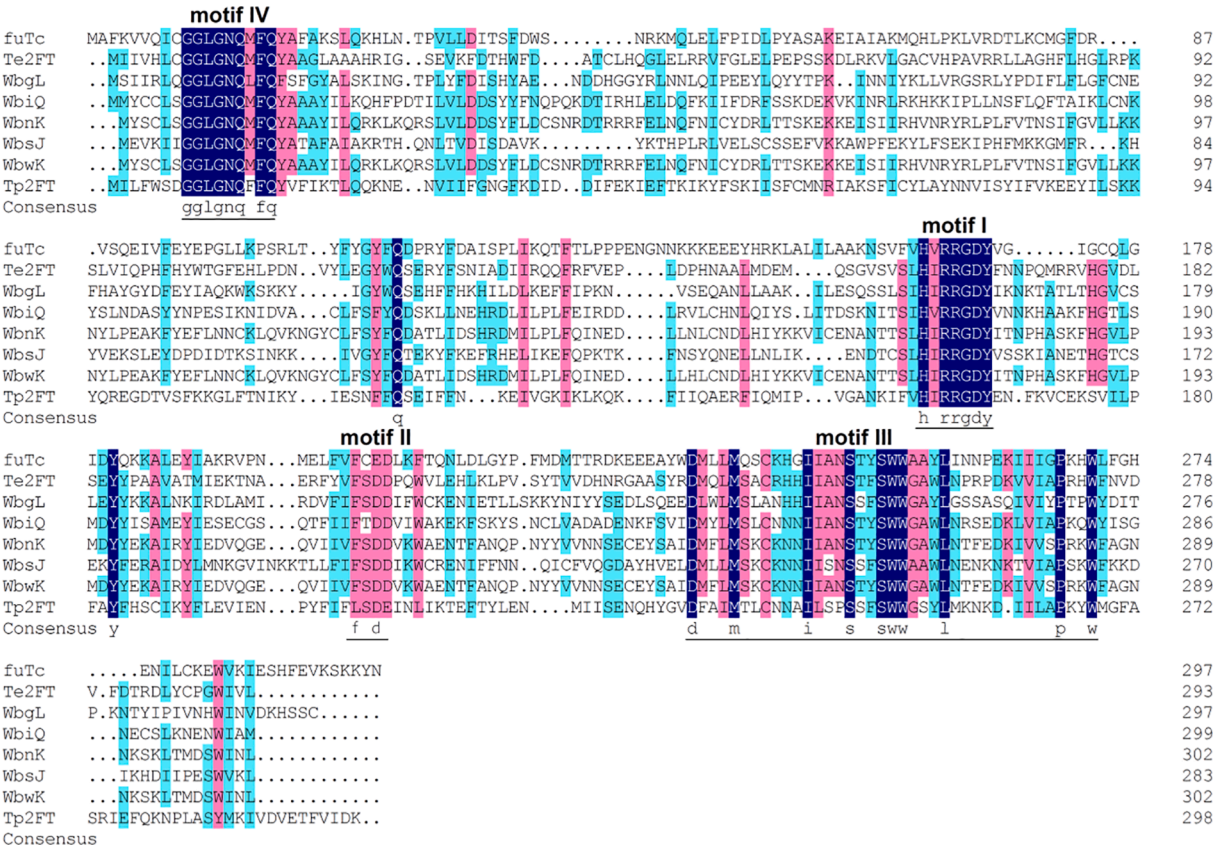

Fig. 2. Alignment of Tp2FT (GenBank: AEF83667.1), *H. pylori* FutC (UniProtKB: A4L7J1), *T. elongatus* Te2FT (UniProtKB: Q8DK72, GenBank: BAC08546.1), *E. coli* O127:K63 WbiQ (UniProtKB: Q5J7C6), *E. coli* O86:K62:H2 WbnK (UniProtKB: Q58YV9), *E. coli* O128:B12 WbsJ (UniProtKB: Q6XQ53), *E. coli* O86:B7 WbwK (GenBank: AAO37719.1), and *E. coli* O126 WbgL (UniProtKB: A6M9C2). The sequence alignment of the investigated genes indicates four common motifs (I–IV). The highly conserved motif I ($H^{160}xR^{162}R^{163}xD^{165}$) suggests a potential binding site for GDP-fucose. Residues R^{162} and D^{165} were indicated to play critical roles in donor binding and enzyme activity.

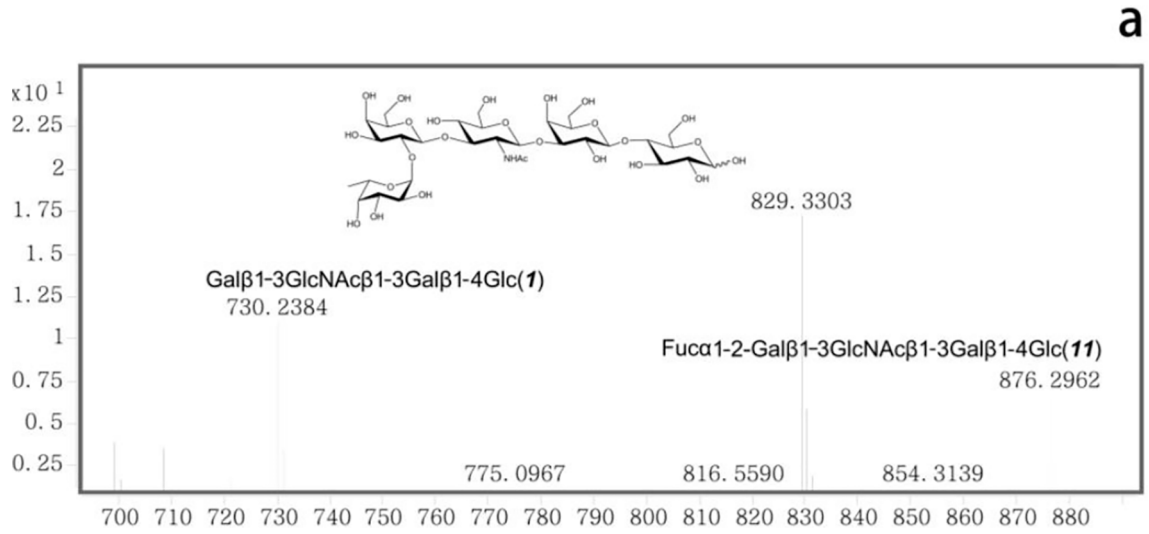

Fig. 3. Mass spectrum of the product synthesized by His_6-Tp α 2FT with Galβ1–3GlcNAcβ1–3Galβ1–4Glc (a); Galβ1–3GalNAcβ$ProN_3$ (b), Galβ1–3GalNAcβ$ProN_3$ (c), Galβ1–3GlcNAc α $ProN_3$ (d), and Galβ1–3GlcNAcβ$ProN_3$ (e) as the receptor substrates; ^{1}H- and ^{13}C NMR spectra of LNFP I (f).

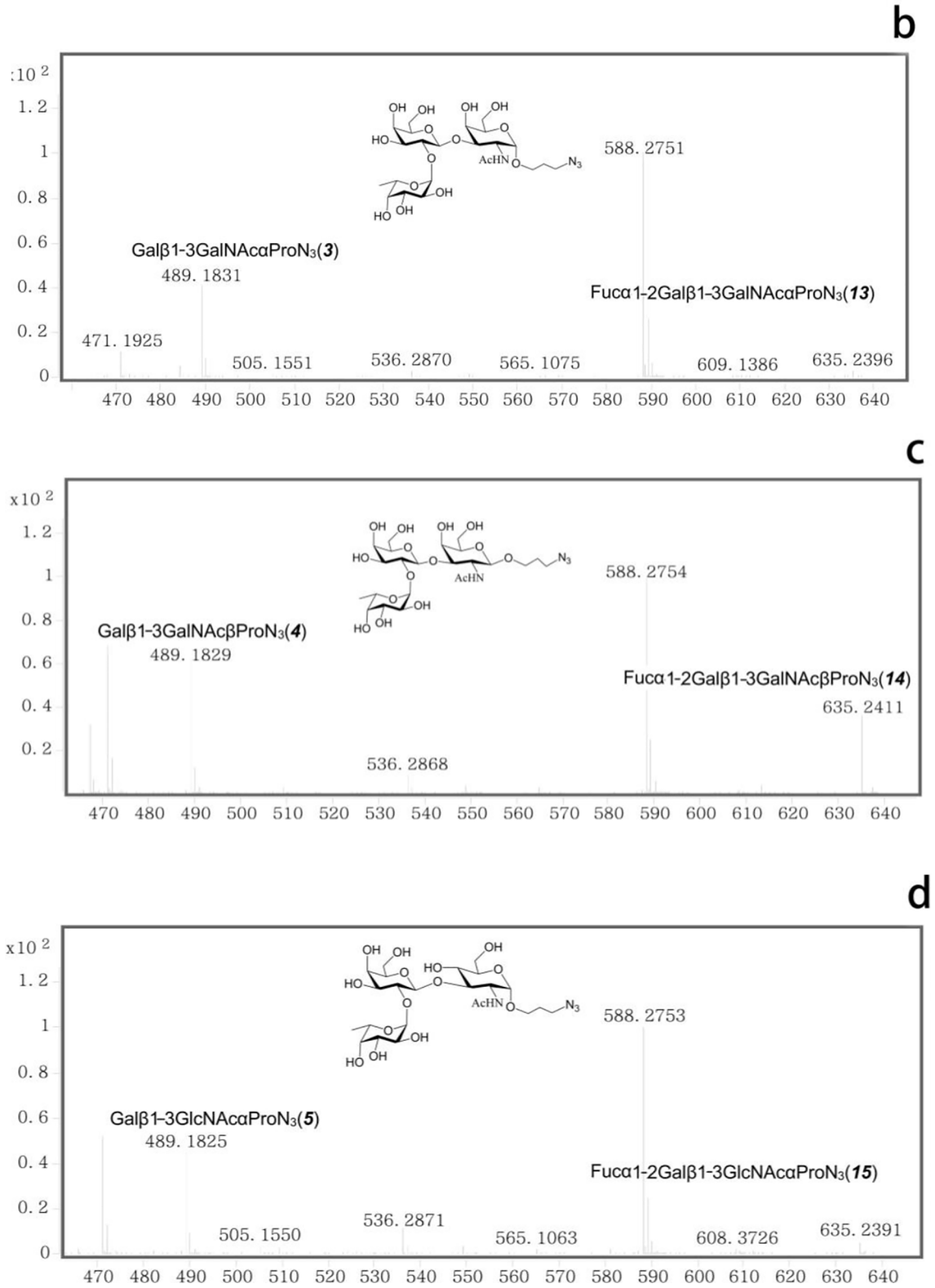

Fig. 3. (*continued*).

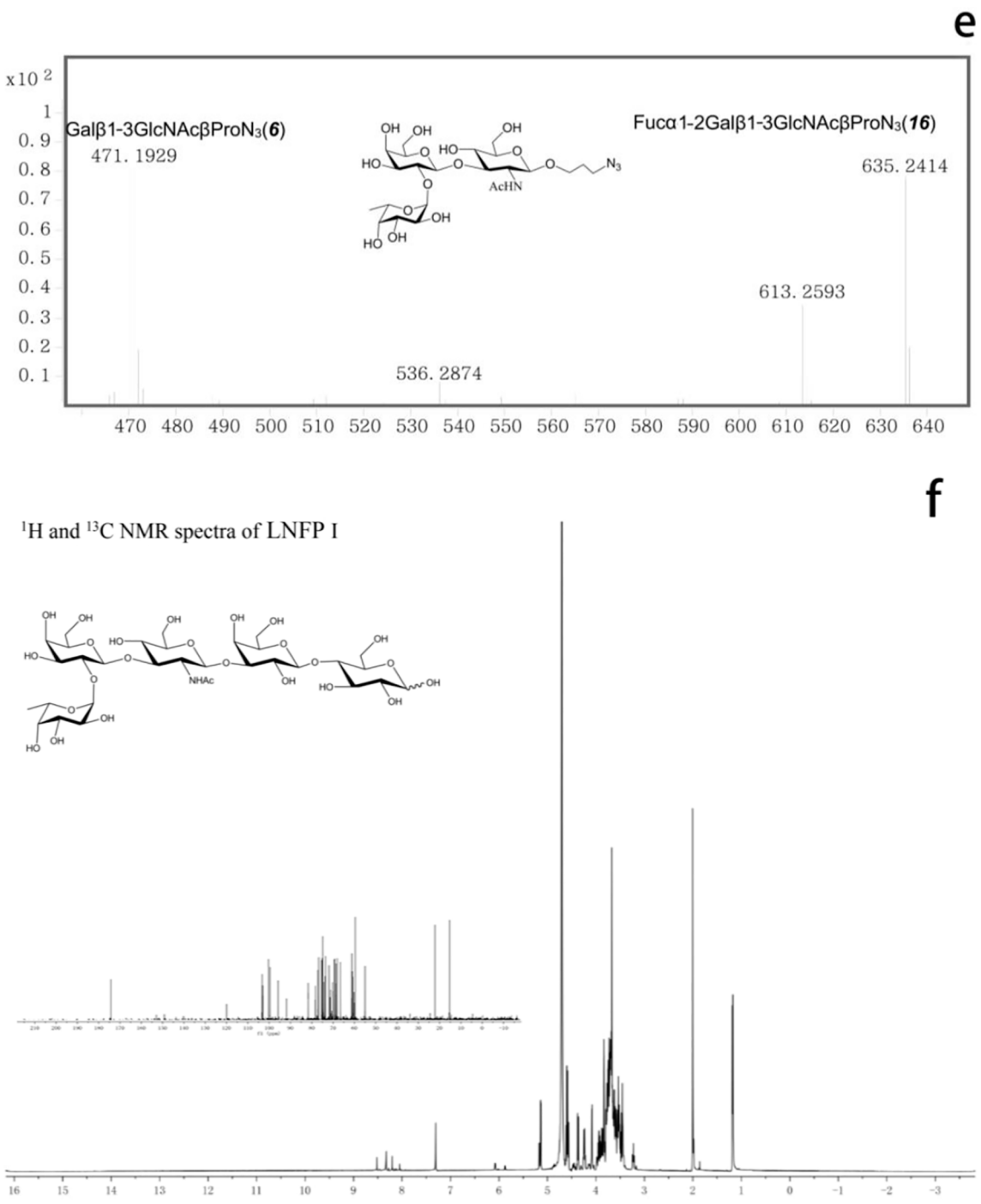

Fig. 3. (*continued*).

purification of proteins were analyzed using 12% sodium dodecyl sulfate–polyacrylamide gel electrophoresis (SDS-PAGE) and stained with Coomassie Brilliant Blue.

2.3. One-pot multienzyme synthesis of α 1–2-linked fucosides

The following constituents were added to a 200-μL micro-centrifuge tube; 1.5 μL of 10 mM adenosine-triphosphate (ATP), 1.5 μL of 10 mM guanosine-triphosphate (GTP), 1 μL of 10 mM magnesiumchloride ($MgCl_2$), 1 μL of 10 mM L-fucose and 2 μL of recombinase Tp2FT (0.3 μg), dissolved in 1 μL of 10 mM Tris-HCl (pH 8.0) with 1 μL of recombinant L-fucokinase/GDP-fucose pyrophosphorylase (FKP, 0.2 μg) (Yi et al., 2009), 1 μL of *Pasteurella multocida* inorganic pyrophosphatase (PmPpA, 0.2 μg) (Lau et al., 2010), and 1 μL of 10 mM acceptor. The acceptor substrates Galβ1–3GalNAc α $ProN_3$, Galβ1–3GalNAcβ$ProN_3$, Galβ1–3GlcNAc α $ProN_3$, and Galβ1–3GlcNAcβ$ProN_3$ were synthesized as described previously (Yu et al., 2010). The others (Table 1) were purchased from Elicityl (Crolles, France). These constituents were then mixed, centrifuged, and incubated at 37°C for 20 h. After incubation, the same volume of ethanol was added to the mixture, mixed, centrifuged, and then diluted 5 times with ddH_2O before sending for mass spectrometry.

2.4. pH, temperature, and divalent metal ion profiles of His_6-Tp2FT

The prepared reaction mixture of 1 μL of 10 mM GDP-fucose, 1 μL of

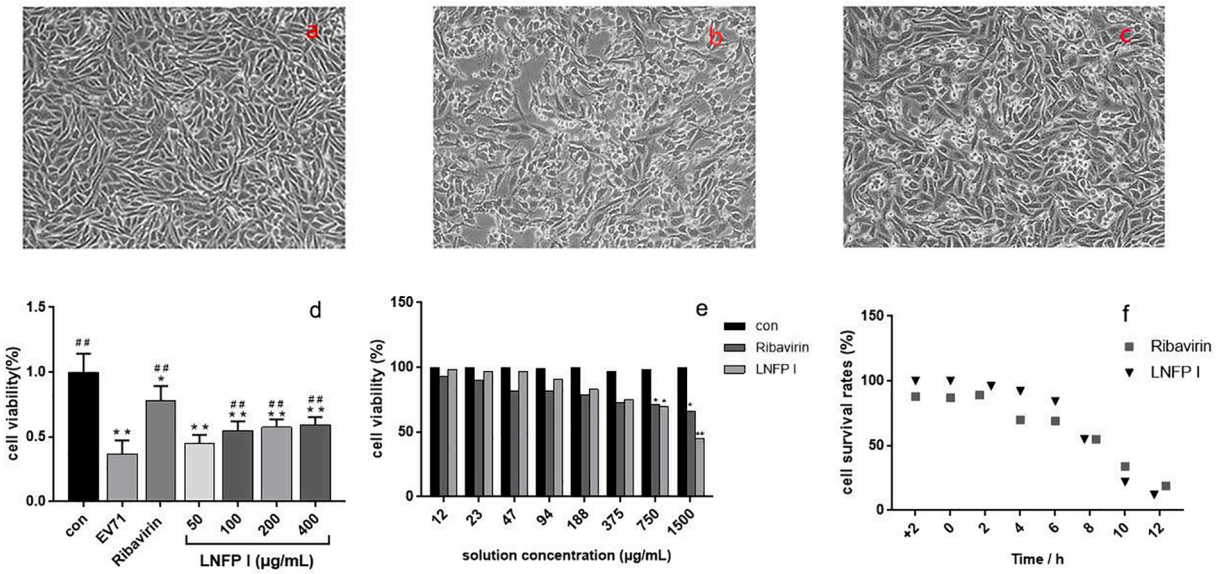

Fig. 4. Effect of LNFP I on Vero and RD cells. (a) Normal cell morphology of RD cells; (b) EV71 infected RD cells for 48 h; (c) The inhibition effect of LNFP I on EV71 virus in RD cells; (d) The inhibition effect of LNFP I on EV71 virus in RD cells; (e) Effect of LNFP I and ribavirin on Vero cells viability; (f) Effect of LNFP I on different stages of EV71 virus infection. Compared with the control group, $^{*}p < 0.05$, $^{**}p < 0.01$; Compared with the LPS group, $^{\#}p < 0.05$, $^{\#\#}p < 0.01$.

10 mM lacto-*N*-tetraose (LNT), 6 μL of purified enzyme His_6-Tp2FT, 1 μL of 10 mM $MgCl_2$, 1 μL of 10 mM Tris-HCl was incubated at same pH (8.0) and different temperatures (15℃, 20℃, 25℃, 30℃, 35℃, 40℃, 45℃, 50℃, 55℃, 60℃) for 5 min, and at same temperature (37℃) and different pH (3.0, 4.0, 5.0, 6.0, 7.0, 8.0, 9.0) 37℃ for 5 min. The pH value of buffer was adjusted with citric acid (pH 3.0–4.0), MES (pH 5.0–6.0) and Tris-HCl (pH 7.0–9.0). The same mixture (except $MgCl_2$) at pH 7.0 was incubated with different concentrations of $MgCl_2$ (1 μL of 5 mM, 10 mM, and 20 mM each), 10 mM EDTA, and 1 μL of 10 mM Tris-HCl at 37℃ for 5 min. The samples were analyzed by a Shimadzu Prominence LC-20A system equipped with a membrane online degasser, a temperature control unit, and a fluorescence detector. A reverse-phase Premier C18 column (250 × 4.0 mm i.d., 5 μm, Shimadzu) was used. The mobile phase was acetonitrile/water (65:35), 1% formic acid at a flow rate of 0.2 mL/min at 40℃ (Zhong et al., 2022). Glycan-containing fractions were analyzed by mass spectrometry.

2.5. Purification and detection of LNFP I

The purity of LNFP I was improved by purifying the synthetic product. For this purpose, 2 g of activated charcoal was added to a 50 mL centrifuge tube and washed twice with ethanol (absolute ethanol or 90% ethanol, 30 mL). The tube was then centrifuged at 15,294×*g* for 30 min and the supernatant was decanted. The process was repeated in which the ethanol was added to wash the activated charcoal, centrifuged, and decanted. The distilled water was then added to the tube and mixed thoroughly by inverting the tube, which was then followed by centrifugation for 30 min. The supernatant was decanted and the tube was left at room temperature for 30 min to evaporate any residues of ethanol. The crude LNFP I (100 mg) was added to the tube with 30 mL of distilled water and mixed thoroughly. The tube was then incubated in a shaking incubator for 1–2 h at 37℃. It was then centrifuged at 15,294×*g* for 30 min to settle down the activated charcoal and the supernatant was decanted. Finally, 50% methanol (30 mL) was added to the tube and mixed thoroughly by inverting the tube, followed by centrifugation for 30 min. The supernatant was collected and passed through a filter to remove any activated charcoal particles. The process was repeated. The filtered solution was then lyophilized to obtain pure white solid LNFP I. The fucosylation of LNT successfully produced a fucosylated product Fuc α 1–2Galβ1–3GlcNAcβ1–3Galβ1–4Glc with an excellent yield of 95%. To confirm the integrity of compounds, the purified products were analyzed by Liquid Chromatograph-Mass Spectrometer (LC-MS) (Agilent 1100 LC/MSD Trap XCT) (Engels and Elling, 2014). ^{1}H- and ^{13}C NMR were used for the confirmation of products. The LNFP I product was dissolved in D_2O and lyophilized before the NMR spectra were recorded at 303 K in a 5 mL tube (Pettit et al., 2010).

2.6. Cell culture

The rhabdomyosarcoma (RD), Vero, and RAW264.7 cells were cultured in Dulbecco's Modified Eagle's Medium (DMEM) (Gibco, Australla) with 10% heat-inactivated fetal bovine serum (FBS) (Gibco, Australla) and 1% penicillin/streptomycin solution (PS). The growth cycle of cells was 6–7 days in 5% CO_2 at 37℃.

2.7. The infection of EV71 virus

The single layers of cells in the plate were washed with Phosphate Buffered Saline (PBS) to clean the plate. Then the serum-free DMEM medium, containing virus-infected cells, was incubated at 37℃ for about 2 h. The fresh DMEM medium, containing 2% FBS, was replaced with the supernatant and incubated at 37℃ with 5% CO_2 for 12 h. The supernatant and cells were then placed in the refrigerator at −80℃, frozen and thawed for three times and then centrifuged (4℃, 2447×*g*, and 10 min). The supernatant was filtered out using 0.22 μm filter. The serial dilutions (10-folds) of viral supernatant were seeded into a 96-well plate having an appropriate cell culture fluid. The culture plate was incubated for 7 days at 37℃ in a 5% CO_2 atmosphere, and the cytopathology of cells was examined under an optical microscope.

2.8. Inhibition effect of LNFP I on EV71 in RD cells

The RD cells adhered to the wells of the 96-well plate as previously described (Gao et al., 2022). The different concentrations of LNFP I (50, 100, 200, and 400 μg/mL) and ribavirin (100 μg/mL) were added into the wells. The EV71 viral solution was added after 2 h of incubation. After 24 h of incubation, the CCK-8 kits (Beyotime, Shanghai, China) were used to measure the absorbance of the solution.

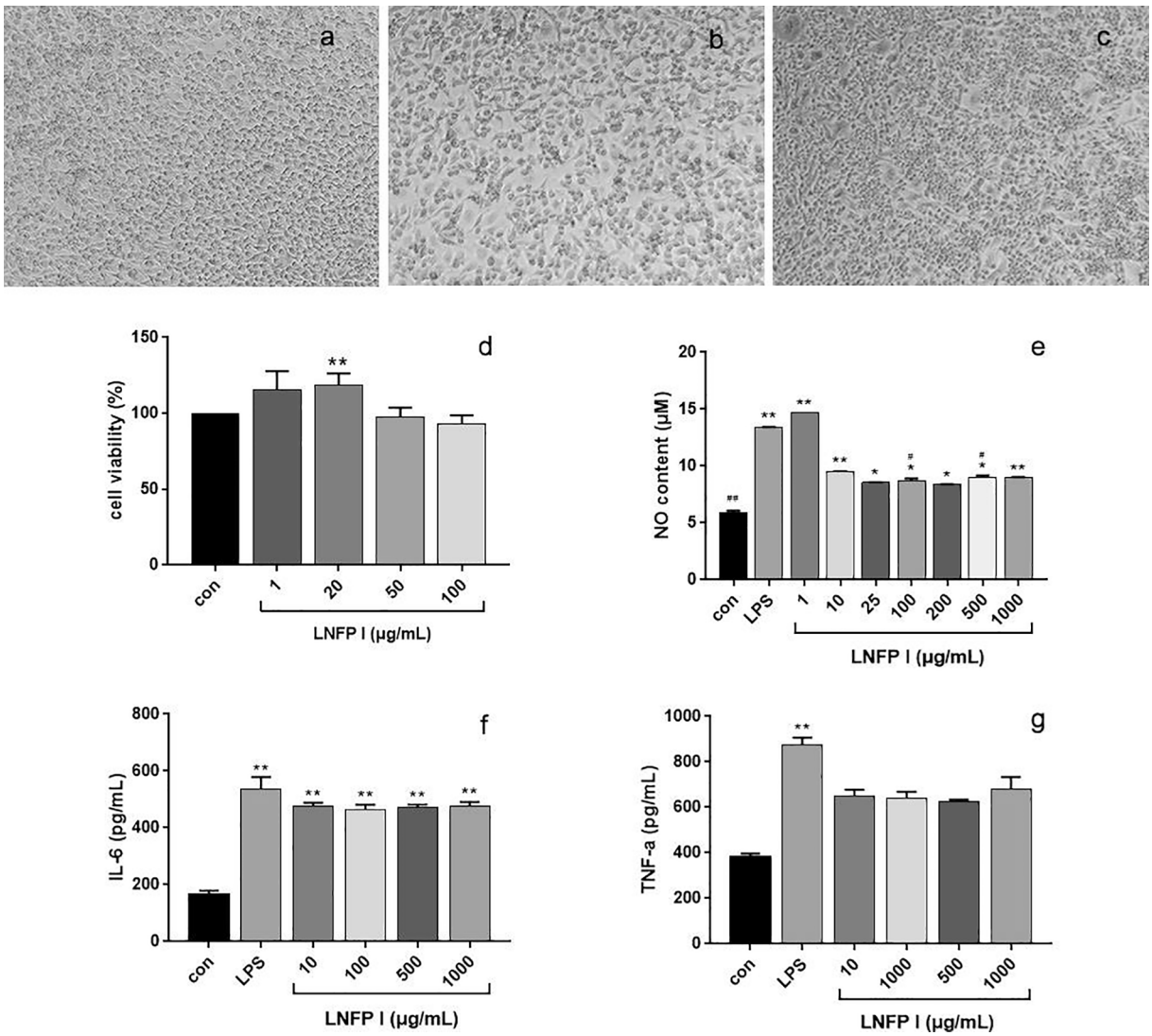

Fig. 5. Effects of LNFP I on RAW264.7 cells. (a) Normal cell morphology of RAW264.7 cells; (b) Cell morphology of LPS-stimulated RAW264.7 cells; (c) Cell morphology of RAW264.7 cells by LNFP I treated; (d) Effect of LNFP I on viability of RAW264.7 cells; (e) Effect of LNFP I on the release of NO of RAW264.7 cells stimulated by LPS solution; (f, g) Effects of LNFP I treatment on the levels of IL-6 and TNF- α. The values were expressed as mean SD (n = 3). Compared with control group, $^{*}p < 0.05$, $^{**}p < 0.01$; Compared with LPS group, $^{\#}p < 0.05$, $^{\#\#}p < 0.01$.

2.9. Effect of LNFP I on the viability of Vero cells

The Vero cells at their logarithmic growth stage were centrifuged at 106 × *g* for 5 min, and re-suspended in DMEM medium with 10% FBS and 1% PS (1×10^4 cells/mL). The cell suspension was seeded in 96-flat-well plates (100 μL/well), allowed to grow for 6 h to adhere the cells on the wells of plates (37℃, 5% CO_2). Then, the different concentrations of LNFP I solution (1, 20, 50, and 100 μg/mL) were added to each well. After incubation for 24 h, the CCK-8 solution was added into wells and incubated them for 4 h. The absorbance of the solution was measured at 450 nm to calculate the viability of cells. The same method was used to determine the effects of different concentrations of LNFP I solution (12, 23, 47, 94, 188, 375, 750, and 1500 μg/mL) on the viability of Vero cells.

2.10. Effect of LNFP I on EV71 in Vero cells

The Vero cells adhered to the wells of the on 96-well plate, as previously described. The EV71 viral solution (10 μL) was added to each well. After 2, 4, 6, 8, 10 and 12 h, the same concentrations (80 μg/mL) of LNFP I and ribavirin were added. After 24 h of incubation, CCK-8 kits (Beyotime, Shanghai, China) were used to measure the cellular activity, and the cell survival rates were calculated.

2.11. Effect of LNFP I on LPS-stimulated RAW264.7 cells

The RAW264.7 cells adhered to the wells of the 96-well plate, as previously described. The different concentrations (1, 5, 10, and 20 μg/mL) of LPS solution (L8880, Solarbio, Beijing, China) were added into wells. After 24 h of incubation, the nitric oxide (NO) content in the cell culture medium was measured. The optimal concentration of LPS solution was selected for the stimulation of RAW264.7 cells to establish an inflammatory model. A total of 100 μL of LNFP I solution with different concentrations (1, 10, 25, 100, 200, 500, and 1000 μg/mL) was added to each well. After incubation for 24 h, the cells were observed under an inverted microscope, and the supernatant was collected. Finally, the NO content was detected using a nitric oxide detection kit (S0021, Beyotime, Shanghai, China) and the levels of Interleukin- 6 (IL-6), Tumor Necrosis Factor (TNF-α) were detected using ELISA test kits (Jiancheng Bioengineering Institute, Nanjing, China).

2.12. Statistical analyses

All the experimental data were expressed as means ± standard deviation (SD). All the statistical analyses were assessed using SPSS (ANVOA, SPSS 25.0) and $p < 0.05$ was considered statistically significant.

3. Results and discussion

3.1. Cloning, expression and purification of His_6-Tp2FT

The experimental results showed that Tp2FT (GenBank accession number AEF83667.1) sequence comparison presented lower level of amino acid identity compared to other reported functionally α 2FTs, exhibiting good novelty. At the same time, the amino acid sequences of Tp2FT were compared with these 7 strains α 2FTs (Fig. 2). The sequence alignment revealed that Tp2FT contained several conserved motifs I–Ⅳ which were identified to be the catalytic sites. The highly conserved motif I containing H^{160}*$R^{162}R^{163}$*D^{165} provided the potential binding site of enzymatic synthesis of fucosylated oligosaccharides (Ihara et al., 2007). The His-tag itself had a small molecular mass, low immunogenicity, and was compatible with the mechanism of transcription and translation in bacteria. The mild conditions of purification had little impact on proteins. The Tp2FT was cloned as an N-His_6-tagged recombinant protein (His_6-Tp2FT) in the pET15b vector. As shown in **Fig. S1**, the Ni^{2+}-column purified protein exhibited a molecular mass of about 36 kDa in SDS-PAGE. The expression level of His_6-Tp2FT was 5.3 mg/L culture, which was lower than Te2FT but nearly other reported α 2FTs (Engels & Elling, 2014; Zhao et al., 2016; Zhong et al., 2022).

3.2. Synthesis of α 1–2-linked fucosides

The relative activities of His_6-Tp2FT with different acceptors were summarizd in Table 1. Common acceptors for α 2FT other than O-fucosyltransferases are galactosides or fucose on oligosaccharides. A panel of ten glycosides with different lengths, various glycosyl linkages and underlying glycans were tested as potential acceptor substrates for the purified His_6-Tp2FT. The initial substrate specific studies using these acceptor substrates, including lacto-*N*-tetraose (LNT, Galβ1–3GlcNAcβ1–3Galβ1,4Glc, ***1***), lacto-*N*-neotetraose (LNnT, Galβ1–4GlcNAcβ1–3Galβ1–4Glc, ***2***), Galβ1–3GalNAcβProN$_3$ (***3***), Galβ1–3GalNAcβProN3 (***4***), Galβ1–3GlcNAc α ProN$_3$ (***5***), Galβ1–3GlcNAcβProN$_3$ (***6***), lacNAcβ-ProN$_3$ (Galβ1–4GlcNAcβProN$_3$, ***7***), lacβProN3 (Galβ1–4GlcβProN$_3$, ***8***), lactose (Galβ1–4Glc, ***9***), and lactulose (Galβ1–4Fru, ***10***), indicating that His_6-Tp2FT worked well. Among these acceptors, the yield of Fuc α 1–2-Galβ1–3GlcNAcβProN$_3$ (***16***) (94.1%) is much higher than the others. The His_6-Tp2FT was used for the synthesis of oligosaccharides by OPME. Despite the ability of 2FucTs to fucosylate a wide range of oligosaccharides, it distinctly favored type 1 glycans (Galβ1–3GlcNAc-) over type 2 glycans (Galβ1–4GlcNAc-) (Fig. 3**a-e**).

3.3. Biochemical characterization of His-Tp2FT

The optimum temperature, pH, and divalent metal ions with LNT as an acceptor were carried out for studying the α 2FT. The results showed that the His_6-Tp2FT was active within a pH range of 5.0–8.0 with optimum activity at pH 7.0 (**Fig. S2**). As compared to His_6-Te2FT (Zhao et al., 2016), the His_6-Tp2FT was active in a broader pH range. It had good activity within the temperature range of 15–60℃, with the optimum activity at 35–45℃. The α 2FT activity of His_6-Tp2FT did not require divalent metal ions. The enzymatic activity of EDTA group was similar to the control group without metal ions, while both of them were lower than that with metal Mg^{2+}, indicating that the Mg^{2+} had a promoting effect. To a certain extent, the higher concentrations of Mg^{2+} exhibited more obvious effects. The α 2FT activity increased by about two folds at the concentrations of 20 mM $MgCl_2$.

3.4. Preparative enzymatic synthesis of LNFP I

For the verification of the activity of His_6-Tp2FT, the small-scale synthesis of LNFP I was demonstrated. An amount of 50 mg of LNFP I was successfully obtained with an excellent yield of 95% using gel filtration. To confirm its correct linkages and structure, the purified LNFP I was analyzed using ^{1}H- and ^{13}C NMR (Fig. 3**f**).

3.5. Inhibition effect of LNFP I on EV71 in RD cells

After the infection of RD cells with EV71, the cell vitality was significantly reduced. Both ribavirin and LNFP I could inhibit the viral infection, and the cell viabilities in the treatment groups were significantly higher than that of the virus-infected group (Fig. 4**a-d**). The fucose on LNFP I might be the binding site for interaction with EV71 (Morozov et al., 2018). The EV71 has four main binding sites, including scavenger receptor class B member 2, P-selectin glycoprotein ligand-1, sialylated glycans and annexin A2 (Jiao et al., 2014; Yang, Chuang, & Yang, 2009; Yang et al., 2011). Therefore, the LNFP I improved cellular viability via competing with EV71 to bind to these target cells in this study. According to the previous studies, the inhibitory effect of LNFP I on EV71 was better than ribavirin possibly due to the potential side effects of ribavirin (Dusheiko, Nelson, & Reddy, 2008; Fang, Srivastava, & Lin, 2003).

3.6. Inhibition effect of LNFP I on EV17-infected Vero cells

Ribavirin is clinically used for the treatment of mild HFMD and can inhibit viral replication in a variety of ways (Li et al., 2018). The viral mRNA (guanine-N'-)-methyltransferase is inhibited by ribavirin 5′-trihosphate or ribavirin, which can inhibit the virus polymerase in the initiation of primary transcription (Zhurilo et al., 2018). LNFP I has less toxic to Vero cells. The viability of Vero cells was significantly reduced at the high concentration of 1500 μg/mL LNFP I solution (Fig. 4**e**). LNFP I could greatly reduce the infection level of EV71 in Vero cells during 2 h before and after infection with EV71. However, after the 6 h of infection, the inhibition by LNFP I was gradually weakened, and the viral replication of EV71 began to increase. The inhibition by LNFP I decreased significantly after 10 h of infection (Fig. 4**f**). It had more advantages for the prevention of EV71 infection and its early treatment of infection. Gao et al. (2020) found that suppressor of the cytokine signaling (SOCS) may promote EV71 virus infection. In the early stage, the induction of SOCS gene transcription was an interferon independent manner and could be blocked by the NF-κB inhibitor (Chmiest et al., 2016). When EV71 virus infects Vero cells, the signaling function of NF-κB pathway responds rapidly and the viral RNA replicates in large quantities, which result in cell ruptures and inactivation. Therefore, LNFP I can reduce the level of SOCS in living cells, but only slow down the virus replication after several hours of infection.

3.7. Effect of LNFP I on the viability of RAW264.7 cells

The normal RAW264.7 cells were round, with bright edges and tight growth between the cells. In terms of cellular shape, a few cells had a low degree of prosthetic foot extensions (Fig. 5**a**). As compared to the normal cells, the LPS-stimulated RAW264.7 cells showed irregular shapes, protruded a large number of pseudopodia, significant increase in the in-between spaces, and reduction in number (Fig. 5**b**). The LNFP I treatment significantly reduced the branching of the cells, contracted pseudopodia, restored the cellular morphology to normal, and increased the cell numbers (Fig. 5**c**). As compared to the control group, the LNFP I had no obvious side effects on the viability of RAW264.7 cells, but significantly increased the cell viability at a concentration of 20 μg/mL (Fig. 5**d**). It means that the LNFP I had lower cytotoxicity and promoted cellular proliferation. The *in-vitro* study of LPS-stimulated macrophages is a good model for studying the inflammatory response (Kim et al.,

2008). LPS can specifically activate the NF-κB pathway and drive the expression of pro-inflammatory cytokines TNF- α and IL-6, which resulting in inflammatory response (Zhang et al., 2019). Upon activation by external stimulus, the macrophages will produce a large amount of NO, further inducing the production of inflammatory cytokines. The NO, IL-6, and TNF- α are considered to be the most important inflammatory mediators, which can mediate the immune responses and stimulate living macrophages (Dai et al., 2009; Yang et al., 2013). After the stimulation of RAW264.7 cells with LPS, the contents of NO in the cell culture medium all increased significantly. Compared with the LPS group, NO release of cells pretreated with different concentrations of LNFP I (10–1000 μg/mL) was significantly reduced ($p < 0.05$) in a dose-independent manner (Fig. 5**e**). LNFP I inhibited inflammatory cytokines IL-6 and TNF- α, and the difference in anti-inflammatory efficacy between groups gradually decreased (Fig. 5**f-g**). These results are consistent with the previous response rule of pro-inflammatory medium NO to LNFP I. It confirms that LNFP I can reduce the content of anti-inflammatory factors IL-6 and TNF- α by inhibiting NO release and alleviating cellular inflammation. Therefore, the goal of the suppression of inflammation could be achieved with a small LNFP I dose. Zhang et al. (2019) reported that NO production in RAW264.7 macrophages might be induced by human milk oligosaccharides instead of LPS. Thus, high concentrations of LNFP I may slightly lead to NO release, making it difficult to exhibit dose-dependence.

4. Conclusion

In this study, a novel α 1–2-fucosyltransferase was cloned from *Treponema primitia* and expressed as a recombinant protein. It was used to catalyze one-pot multienzyme synthesis of lacto-*N*-fucopentaose-I. LNFP I exhibited effective anti-inflammatory and anti-EV71 effects. It not only reduced the contents of inflammatory cytokines during the inflammatory response, but also effectively inhibited the synthesis of the proliferation of EV71 in a dose-dependent manner. It had low toxic effects on cells and inhibited the EV71 infection in its early stage, thereby using in infant nutrition and providing a novel therapeutic target for the prevention of HFMD.

CRediT authorship contribution statement

Yuanyuan Liu: Investigation, Formal analysis, Writing – original draft. **Aijun Tong:** Investigation, Formal analysis, Writing – original draft. **Xiaoxiang Gao:** Formal analysis. **Sinan Yuan:** Formal analysis. **Ruting Zhong:** Writing – review & editing. **Chao Zhao:** Conceptualization, Writing – original draft, Writing – review & editing.

Declaration of Competing Interest

The authors declare that they have no known competing financial interests or personal relationships that could have appeared to influence the work reported in this paper.

Acknowledgments

The project was funded by Key Project of the Natural Science Foundation of Fujian Province (2020J02032) and Fujian 'Young Eagle Program' Youth Top Talent Program. This work was also supported by Project of Excellent Master Degree Thesis and Double First-Class Construction Plan (KSYLX013) of Fujian Agriculture and Forestry University.

Appendix A. Supplementary data

Supplementary data to this article can be found online at https://doi.org/10.1016/j.fochx.2022.100273.

References

Baumgärtner, F., Seitz, L., Sprenger, G. A., & Albermann, C. (2013). Construction of *Escherichia coli* strains with chromosomally integrated expression cassettes for the synthesis of 2'-fucosyllactose. *Microbial Cell Factories, 12*, 40.

Castanys-Muñoz, E., Martin, M. J., & Prieto, P. A. (2013). 2'-fucosyllactose: An abundant, genetically determined soluble glycan present in human milk. *Nutrition Reviews, 71*(12), 773–789.

Chmiest, D., Sharma, N., Zanin, N., Viaris de Lesegno, C., Shafaq-Zadah, M., Sibut, V., et al. (2016). Spatiotemporal control of interferon-induced JAK/STAT signalling and gene transcription by the retromer complex. *Nature Communications, 7*(1), 13476.

Dai, R., Phillips, R. A., Karpuzoglu, E., Khan, D., & Ahmed, S. A. (2009). Estrogen regulates transcription factors STAT-1 and NF-κB to promote inducible nitric oxide synthase and inflammatory responses. *Journal of Immunology, 183*(11), 6998–7005.

Derya, S. M., Spiegel, H., Hanisch, F.-G., Morozov, V., Schroten, H., Jennewein, S., et al. (2020). Biotechnologically produced fucosylated oligosaccharides inhibit the binding of human noroviruses to their natural receptors. *Journal of Biotechnology, 318*, 31–38.

Dusheiko, G., Nelson, D., & Reddy, K. R. (2008). Ribavirin considerations in treatment optimization. *Antiviral Therapy, 13*(1), 23–30.

Engels, L., & Elling, L. (2014). Wbgl: A novel bacterial α1,2-fucosyltransferase for the synthesis of 2'-fucosyllactose. *Glycobiology, 24*(2), 170–178.

Fang, C., Srivastava, P., & Lin, C.-C. (2003). Effect of ribavirin, levovirin and viramidine on liver toxicological gene expression in rats. *Journal of Applied Toxicology, 23*(6), 453–459.

Gao, W., Hou, M., Liu, X., Li, Z., Yang, Y., & Zhang, W. (2020). Induction of SOCS expression by EV71 infection promotes EV71 replication. *BioMed Research International, 2020*, 1–9.

Gao, X., Qiu, Y., Gao, L., Zhang, L., Li, X., Liu, Y., et al. (2022). Fucosylated oligosaccharide Lacto-*N*-fucopentaose I ameliorates enterovirus 71 infection by inhibiting apoptosis. *Food Chemistry: X, 13*, Article 100244.

Gao, X., Wu, D., Wen, Y., Gao, L., Liu, D., Zhong, R., et al. (2020). Antiviral effects of human milk oligosaccharides: A review. *International Dairy Journal, 110*, 104784.

Gnoth, M. J., Kunz, C., KinneSaffran, E., & Rudloff, S. (2000). Human milk oligosaccharides are minimally digested in vitro. *Journal of Nutrition, 130*(12), 3014–3020.

Ihara, H., Ikeda, Y., Toma, S., Wang, X. C., Suzuki, T., Gu, J. G., et al. (2007). Crystal structure of mammalian alpha1,6-fucosyltransferase, FUT8. *Glycobiology, 17*(5), 455–466.

Jiao, X.-Y., Guo, L.i., Huang, D.-Y., Chang, X.-L., & Qiu, Q.-C. (2014). Distribution of EV71 receptors SCARB2 and PSGL-1 in human tissues. *Virus Research, 190*, 40–52.

Kim, Y., Zhao, R. J., Park, S. J., Lee, J. R., Cho, I. J., Yang, C. H., et al. (2008). Anti-inflammatory effects of liquiritigenin as a consequence of the inhibition of NF-κB-dependent iNOS and proinflammatory cytokines production. *British Journal of Pharmacology, 154*(1), 165–173.

Lau, K., Thon, V., Yu, H., Ding, L., Chen, Y., Muthana, M. M., et al. (2010). Highly efficient chemoenzymatic synthesis of beta1–4-linked galactosides with promiscuous bacterial beta1-4-galactosyltransferases. *Chemical Communications, 46(33)*, 6066–606.

Lee, W.-H., Pathanibul, P., Quarterman, J., Jo, J.-H., Han, N. S., Miller, M. J., et al. (2012). Whole cell biosynthesis of a functional oligosaccharide, 2'-fucosyllactose, using engineered *Escherichia coli*. *Microbial Cell Factories, 11*(1), 1–9.

Li, M., Liu, X. W., Shao, J., Shen, J., Jia, Q., Wen, Y.i., et al. (2008). Characterization of a novel alpha1,2-fucosyltransferase of *Escherichia coli* O128_b12 and functional investigation of its common motif. *Biochemistry, 47*(1), 378–387.

Li, M., Shen, J., Liu, X. W., Shao, J., Yi, W., Chow, C. S., et al. (2008). Identification of a new 1,2-fucosyltransferase involved in O-antigen biosynthesis of *Escherichia coli* O86_b7 and formation of H-type 3 blood group antigen. *Biochemistry, 47*(44), 11590–11597.

Li, P., Yu, J., Hao, F., He, H. Y., Shi, X. Y., Hu, J., et al. (2018). Discovery of potent EV71 capsid inhibitors for treatment of HFMD. *ACS Medicinal Chemistry Letters, 8*, 841–846.

Liu, X., Xie, J. H., Jia, S., Huang, L. X., Wang, Z. J., Li, C., et al. (2017). Immunomodulatory effects of an acetylated *Cyclocarya paliurus* polysaccharide on murine macrophages RAW264.7. *International Journal of Biological Macromolecules, 98*, 576–581.

Lyu, K.e., Wang, G.-C., He, Y.-L., Han, J.-F., Ye, Q., Qin, C.-F., et al. (2015). Crystal structures of enterovirus 71 (EV71) recombinant virus particles provide insights into vaccine design. *Journal of Biological Chemistry, 290*(6), 3198–3208.

Meints, L. M., Poston, A. W., Piligian, B. F., Olson, C. D., Badger, K. S., Woodruff, P. J., et al. (2017). Rapid one-step enzymatic synthesis and all-aqueous purification of trehalose analogues. *Journal of Visualized Experiments, 120*, 54485.

McMinn, P. C. (2012). Recent advances in the molecular epidemiology and control of human enterovirus 71 infection. *Current Opinion in Virology, 2*(2), 199–205.

Morozov, V., Hansman, G., Hanisch, F.-G., Schroten, H., & Kunz, C. (2018). Human milk oligosaccharides as promising antivirals. *Molecular Nutrition & Food Research, 62*(6), 1700679.

Pettit, N., Styslinger, T., Zhen, M., Han, W., Zhao, G., & Peng, G. W. (2010). Characterization of wbiq: An 1,2-fucosyltransferase from *Escherichia coli* O127:K63 (b8), and synthesis of h-type 3 blood group antigen. *Biochemical & Biophysical Research Communications, 402*(2), 190–195.

Ruiz-Palacios, G. M., Cervantes, L. E., Ramos, P., Chavez-Munguia, B., & Newburg, D. S. (2003). *Campylobacter jejuni* binds intestinal H(O) antigen (Fuc alpha 1, 2Gal beta 1, 4GlcNAc), and fucosyloligosaccharides of human milk inhibit its binding and infection. *Journal of Biological Chemistry, 278*(16), 14112–14120.

Seydametova, E., Yu, J., Shin, J., Park, Y., Kim, C., Kim, H., et al. (2019). Search for bacterial 1,2-fucosyltransferases for whole-cell biosynthesis of 2'-fucosyllactose in recombinant *Escherichia coli*. *Microbiological Research*, 35–42.

Smyth, M. S., & Martin, J. H. (2002). Picornavirus uncoating. *Molecular Plant Pathology, 55*, 214.

Sprenger, G. A., Baumgärtner, F., & Albermann, C. (2017). Production of human milk oligosaccharides by enzymatic and whole-cell microbial biotransformations. *Journal of Biotechnology, 258*, 79–91.

Stein, D., Lin, Y. N., & Lin, C. H. (2008). Characterization of *Helicobacter pylori* 1,2-fucosyltransferase for enzymatic synthesis of tumor-associated antigens. *Advanced Synthesis & Catalysis, 350*(14–15), 2313–2321.

Wang, G., Boulton, P. G., Chan, N. W. C., Palcic, M. M., & Taylor, D. E. (1999). Novel *Helicobacter pylori* α1,2-fucosyltransferase, a key enzyme in the synthesis of lewis antigens. *Microbiology, 145*(11), 3245–3253.

Wilson, A. E., Feng, X., Ono, N. N., Holland, D., Amir, R., & Tian, L.i. (2017). Characterization of a UGT84 family glycosyltransferase provides new insights into substrate binding and reactivity of galloylglucose ester-forming UGTs. *Biochemistry, 56*(48), 6389–6400.

Xiao, Z., Guo, Y., Liu, Y., Li, L., Zhang, Q., Wen, L., et al. (2016). Chemoenzymatic synthesis of a library of human milk oligosaccharides. *The Journal of Organic Chemistry, 81*(14), 5851–5865.

Yang, B., Chuang, H., & Yang, K. D. (2009). Sialylated glycans as receptor and inhibitor of enterovirus 71 infection to DLD-1 intestinal cells. *Journal of Virology, 6*(1), 141.

Yang, J. H., Kim, S. C., Shin, B. Y., Jin, S. H., Jo, M. J., Jegal, K. H., et al. (2013). O-methylated flavonol isorhamnetin prevents acute inflammation through blocking of NF-κB activation. *Food and Chemistry Toxicology, 59*, 362–372.

Yang, S.-L., Chou, Y.-T., Wu, C.-N., & Ho, M.-S. (2011). Annexin II binds to capsid protein VP1 of enterovirus 71 and enhances viral infectivity. *Journal of Virology, 85*(22), 11809–11820.

Yi, W., Liu, X., Li, Y., Li, J., Xia, C., Zhou, G., et al. (2009). Remodeling bacterial polysaccharides by metabolic pathway engineering. *Proceedings of the National Academy of Sciences of the United States of America, 106*(11), 4207–4212.

Ye, J., Xia, H., Sun, N.a., Liu, C.-C., Sheng, A., Chi, L., et al. (2019). Reprogramming the enzymatic assembly line for site-specific fucosylation. *Nature Catalysis, 2*(6), 514–522.

Yu, H., Thon, V., Lau, K., Cai, L., Chen, Y., Mu, S., et al. (2010). Highly efficient chemoenzymatic synthesis of β1-3-linked galactosides. *Chemical Communications, 46*(40), 7507.

Zhang, L., & Wang, C.-C. (2014). Inflammatory response of macrophages in infection. *Hepatobiliary & Pancreatic Diseases International, 13*(2), 138–152.

Zhang, W. Y., Yan, J. Y., Wu, L. H., Yu, Y., Ye, R. D., Zhang, Y., et al. (2019). *In vitro* immunomodulatory effects of human milk oligosaccharides on murine macrophage RAW264.7 cells. *Carbohydrate Polymers, 207*, 230–238.

Zhao, C., Wu, Y., Liu, X., Liu, B., Cao, H., Yu, H., et al. (2017). Functional properties, structural studies and chemo-enzymatic synthesis of oligosaccharides. *Trends in Food Science & Technology, 66*, 135–145.

Zhao, C., Wu, Y. J., Yu, H., Shah, I. M., Li, Y. H., Zeng, J., et al. (2016). The one-pot multienzyme (OPME) synthesis of human blood group H antigens and a human milk oligosaccharide (HMOS) with highly active *Thermosynechococcus elongates* α1-2-fucosyltransferase. *Chemical Communications, 52*(20), 3899–3902.

Zhong, R., Gao, L., Chen, Z., Yuan, S., Chen, X., & Zhao, C. (2022). Chemoenzymatic synthesis of fucosylated oligosaccharides using *Thermosynechococcus* α1-2-fucosyltransferase and their application in the regulation of intestinal microbiota. *Food Chemistry: X, 12*, Article 100152.

Zhurilo, N. I., Chudinov, M. V., Matveev, A. V., Smirnova, O. S., Konstantinova, I. D., Miroshnikov, A. I., et al. (2018). Isosteric ribavirin analogues: Synthesis and antiviral activities. *Bioorganic & Medicinal Chemistry Letters, 28*(1), 11–14.